

Constraints on future changes in climate and the hydrologic cycle

Myles R. Allen* & William J. Ingram†

*Department of Physics, University of Oxford, Parks Road, Oxford OX1 3PU, UK (e-mail: myles.allen@physics.ox.ac.uk)

†The Hadley Centre, Met Office, London Road, Bracknell RG12 2SZ, UK (e-mail: william.ingram@metoffice.com)

What can we say about changes in the hydrologic cycle on 50-year timescales when we cannot predict rainfall next week? Eventually, perhaps, a great deal: the overall climate response to increasing atmospheric concentrations of greenhouse gases may prove much simpler and more predictable than the chaos of short-term weather. Quantifying the diversity of possible responses is essential for any objective, probability-based climate forecast, and this task will require a new generation of climate modelling experiments, systematically exploring the range of model behaviour that is consistent with observations. It will be substantially harder to quantify the range of possible changes in the hydrologic cycle than in global-mean temperature, both because the observations are less complete and because the physical constraints are weaker.

Climate prediction is about quantifying risks and probabilities. Changes in rainfall distributions could have far more impact than the more-often-cited risk of global warming, but systematically quantifying the likelihood of such changes is only beginning. We cannot hope to predict the exact climate of 2050, still less the weather on a particular day, but we can assess the relative likelihood of different long-term trends given the constraints provided by observations and physical understanding available today.

Here we will explore the range of possible externally driven changes in the hydrologic cycle that may have taken place over the twentieth century or be in prospect for the twenty-first, emphasizing the question of what can be said about future climate^{1,2}. We will not attempt a comprehensive review of the literature, which is amply provided by the recent Third Assessment Report (TAR) of the Intergovernmental Panel on Climate Change (IPCC)^{3,4}. Instead, we review the present status regarding quantitative estimation of the distribution of likely precipitation changes, and their impact on other aspects of the atmosphere–ocean system, focussing on the evidence provided by the twentieth century and its implications for the next few decades. Evidence from past climates may provide additional constraints, particularly on the more distant future. The interpretation of such data and the challenge of disentangling causes and effects are discussed by Kump on pages 188–190 of this issue.

We will focus on the impact of anthropogenic carbon dioxide, both for reasons of space and because CO₂ is expected to dominate climate change in the coming century⁴. Other anthropogenic factors are probably having significant impacts on the hydrologic cycle, notably various forms of aerosol (see ref. 5, and the review in this issue by Kaufman *et al.*, pages 215–223). Changes are also anticipated^{6–10}, and may have already been detected^{11,12}, in how precipitation is distributed between low- and high-intensity events⁷. Regional details of the precipitation response to greenhouse warming are much less clear, as are hydrologic feedbacks on other aspects of the climate system, notably the strength of the oceanic thermohaline circulation (refs 13, 14, and see review in this issue by Rahmstorf, pages 207–214).

Physical arguments, such as those discussed in the preceding articles, indicate the qualitative changes in the hydrologic cycle expected to result from a variety of external influences. They do not, however, provide much more than order-of-magnitude constraints on the likely size of these changes under anthropogenic climate change (ref. 15, and see review in this issue by Pierrehumbert, pages 191–198). Ideally, forecasts of climate change should be constrained objectively by uncontroversial physical principles, possibly but not necessarily through simulation models, combined with actual climate observations. This approach may already be yielding results for predictions of global-mean temperature^{16–20}, but extending it to regional temperature change or changes in the hydrologic cycle presents new challenges which may require a whole new generation of climate modelling experiments²¹.

Constraints on global-mean temperature change

Anticipating difficulties in placing quantitative constraints on changes in the hydrologic cycle, we shall begin with a better constrained problem to show what can be done. Forecast global-mean temperatures are likely to be better constrained by recent climate observations than almost any other climate variable, both for physical reasons and because the historical temperature record is more accurate than for any other global variable. The constraint of global energy conservation means that the global-mean temperature response to an increase in CO₂ is controlled largely by three basic properties of the climate system: (1) the strength of atmospheric and surface feedbacks, which determine the so-called ‘climate sensitivity’ (equilibrium warming on doubling CO₂); (2) the effective heat capacity of the fraction of the oceans in contact with the atmosphere on short (sub- to inter-annual) timescales; and (3) how heat export to the ocean depths depends on recent changes at the surface.

In the absence of a sudden nonlinear climate change (in, say, ocean circulation) these properties of the climate may be expected to change slowly, if at all, in response to an imposed external forcing. Indeed, they are assumed to be constant in most simple and intermediate prognostic models of climate^{22,23}. Even the most complex climate models suggest that strong nonlinearities are unlikely to be important in

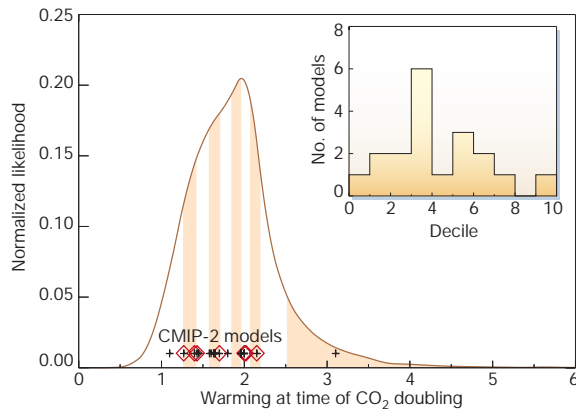


Figure 1 The range of transient climate response (TCR) consistent with recent observed temperature trends, compared to TCRs of some current AOGCMs. The curve shows the warming at the time of CO₂ doubling after an increase in CO₂ concentration of 1% per year (TCR), estimated from comparing an intermediate-complexity model with observations of recent large-scale temperature change, allowing for uncertainty due to internal variability as simulated by an AOGCM (refs 19, 31, with supplementary data supplied by M. D. Webster). The curve has been smoothed for clarity and the vertical bands show equal-area deciles of the distribution. The crosses are the TCRs of the AOGCMs in the CMIP-2 ensemble^{4,25}. Superimposed red diamonds show models used in the TAR summary range of '1.4–5.8 °C warming from 1990 to 2100'. The inset histogram shows how many of the CMIP-2 models fall into each decile of the observationally constrained distribution.

global-mean temperature change over the next half-century or so. For example, in all but one of the 19 coupled atmosphere–ocean general circulation models (AOGCMs) in CMIP-2 (the second Coupled Model Intercomparison Project^{24,25}), an annual 1% compound increase in CO₂ concentrations (a linear increase in radiative forcing) results in a near-linear global-mean temperature response up to and beyond the time of CO₂ doubling after a few years' initial adjustment (ref. 26; and see Fig. 9.3a of ref. 4). Likewise, global-mean precipitation increases roughly linearly in these experiments (Fig. 9.3b of ref. 4), albeit with rather stronger unforced and effective-random variations from year to year.

The net radiative forcing in the CMIP-2 experiments is at the high end of projected anthropogenic changes over the coming decades. Hence current AOGCMs suggest that a strongly nonlinear global-mean temperature response to greenhouse forcing is unlikely over the next few decades at least. In that case, the constraint of global energy conservation means that estimates of past radiative forcing, recent observed near-surface temperature change and the accumulation of heat in the global oceans^{27,28} place objective, albeit still rather weak, constraints on the overall strength of atmospheric feedbacks^{16,17,19,20}. These in turn provide the basis for an objective probabilistic forecast of the temperature response to a given emissions scenario^{18,29,30} of the type we would like, ultimately, to provide for the hydrologic cycle.

The curve in Fig. 1 shows an estimate of the probability distribution of global-mean warming at the time of CO₂ doubling under a scenario of CO₂ concentration increasing by 1% annually (the 'transient climate response', or TCR), which is consistent with recent observations of large-scale surface, atmospheric and oceanic temperature change^{19,31}. Note that this empirical distribution is, if anything, likely to underestimate the range of uncertainty in TCR, as the analysis on which it was based assumed a negligible impact of natural forcing on temperature changes in the twentieth century¹⁷.

The crosses in Fig. 1 show the TCR of the 19 AOGCMs in the CMIP-2 multi-model comparison. If the CMIP-2 models were a

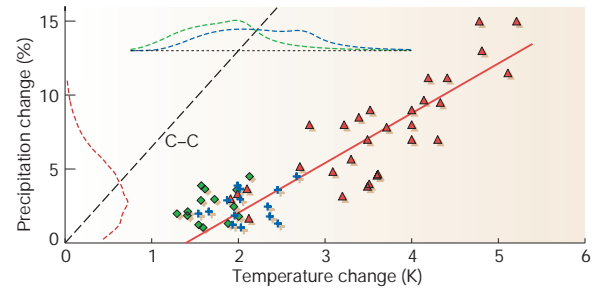


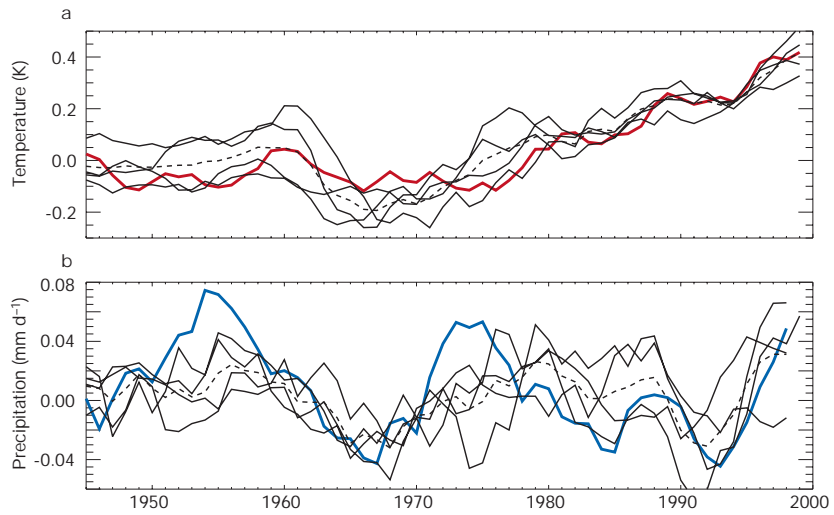
Figure 2 Global-mean temperature and precipitation changes in AOGCM simulations (scatter plots), and probability distributions obtained by requiring consistency with recent observations (curves). Red triangles show global-mean temperature and precipitation changes in a wide range of equilibrium CO₂-doubling experiments with simple thermodynamic ('slab') oceans^{4,45}, with the red line showing the best-fit (least squares) linear relationship. Green diamonds show the same, at the time of CO₂ doubling, for those CMIP-2 models for which the data are available²⁵. Blue crosses are the green diamonds adjusted for disequilibrium in the CMIP-2 runs by adding $\kappa F_0/k_T$ to ΔT (equation (2)), with a single value of $\kappa (=1)$ estimated from the data to remove the bias with the best-fit line through the 'slab' experiments. All these points would lie on the dashed line labelled C–C if precipitation were to follow the Clausius–Clapeyron relation⁴⁴. The green dashed curve is the observationally constrained estimate of the distribution of global-mean temperature change at the time of CO₂ doubling from Fig. 1. The blue curve is the same, but adjusted for disequilibrium like the blue crosses. The red curve shows the distribution of global-mean precipitation changes implied by the blue curve, assuming the same straight-line relationship observed in the 'slab' experiments, with the same amount of scatter (assumed Gaussian).

random sample of possible climate-system behaviour consistent with these observations, then we should expect to find approximately equal numbers of models in each decile (vertical band) of the empirical TCR distribution and a more-or-less flat histogram in the inset panel. Instead, the models are concentrated near the centre of the distribution. Only one model displays a TCR in the uppermost two deciles of the distribution, and this turns out to be fortuitous. Warming accelerates in this particular model³² owing to some form of nonlinearity in the response. The empirical distribution (which assumes that both climate sensitivity and the nature of the ocean response are constant over these timescales) would immediately become much broader if it were to allow for such nonlinearity, pushing even this high-response model down into a relatively low percentile.

If current models underestimate the range of global-mean temperature responses consistent with recent observations, the problem can be expected to be worse for variables such as precipitation, which are not so well constrained by the available data. Hence any assessment of the risk of precipitation change exceeding a given threshold by a given date based solely on the spread of responses of currently available climate models¹⁰ will be underestimated, perhaps by a substantial margin.

Of course, the fact that current climate models do not span the range of responses consistent with recent warming is no indictment of the models: they were not designed to do so. The IPCC TAR was careful not to interpret the spread of the models as a direct measure of uncertainty in climate forecasts, for precisely this reason. Far from being designed to provide random samples of possible representations of the climate system, AOGCMs are generally designed as 'best guess' representations of the system based on a limited set of observations. Hence some clustering of model results towards the centre of the range of physically plausible behaviour should be expected. Because we cannot quantify the extent of this clustering *a priori*, we cannot predict the likelihood of the response in the real world lying above or below the range of model simulations with modelling alone. The only objective probabilistic forecast is provided by the

Figure 3 Changes in observed global-mean temperature (a) and land precipitation (b) over the past 55 years compared with a climate model. The model data are from a four-member initial-condition ensemble of the HadCM3 climate model run with estimates of anthropogenic, solar and volcanic forcing (dashed line shows ensemble mean). Model data were included only where and when observations exist and a five-year running mean was applied to suppress variability such as El Niño, which we would not expect to be coherent between them. Model simulations courtesy of P. Stott, The Met Office, and precipitation data courtesy of M. Hulme, Tyndall Centre^{38,71}.



constraint of consistency with actual climate observations. Can we identify analogous constraints on future changes in the hydrologic cycle?

Constraints on hydrologic indicators

Tropospheric humidity

The distribution of moisture in the troposphere (the part of the atmosphere that is strongly coupled to the surface) is complex, but there is one clear and strong control: moisture condenses out of supersaturated air. This constraint broadly accounts for the humidity of tropospheric air parcels above the boundary layer, because almost all such parcels will have reached saturation at some point in their recent history. Physically, therefore, it has long seemed plausible that the distribution of relative humidity would remain roughly constant under climate change³³, in which case the Clausius–Clapeyron relation implies that specific humidity would increase roughly exponentially with temperature. This reasoning is strongest at higher latitudes where air is usually closer to saturation, and where relative humidity is indeed roughly constant through the substantial temperature changes of the seasonal cycle. For lower latitudes it has been argued that the real-world response might be different (see ref. 34 and references therein). But relative humidity seems to change little at low latitudes under a global warming scenario, even in models of very high vertical resolution³⁵, suggesting this may be a robust ‘emergent constraint’ on which models have already converged.

Consistent with this picture of tropospheric specific humidities rising in line with surface warming and more-or-less unchanged relative humidity, apparently significant increases have been observed in surface^{36–38}, boundary-layer³⁹ and lower- to mid-tropospheric⁴⁰ specific humidity levels over some land regions in the Northern Hemisphere. In the tropics and Southern Hemisphere, *in situ* observations remain sparse and satellite records are too inhomogenous to estimate long-term humidity trends⁴¹. Estimated trends in upper tropospheric humidity — the most important for climate sensitivity, but also the most difficult to observe — are also ambiguous⁴². On shorter timescales, current climate-model simulations of the overall strength of water vapour feedback seem reasonably accurate in the case of the eruption of Mount Pinatubo, with the observed reduction in specific humidity being accompanied by only small changes in relative humidity⁴³.

Equilibrium global-mean precipitation changes

If tropospheric moisture loading is controlled by the constraints of (approximately) unchanged relative humidity and the

Clausius–Clapeyron relation, should we expect a corresponding exponential increase in global precipitation and the overall intensity of the hydrologic cycle as global temperatures rise? This is certainly not what is observed in models. The red triangles in Fig. 2 show the long-term equilibrium global-mean near-surface warming, ΔT , and precipitation increase, ΔP , in response to doubling CO_2 in a number of atmospheric models coupled to ‘slab’ (thermodynamic mixed layer) ocean models^{44,45}. They appear to lie, to a reasonable approximation, on a straight line⁴⁶ with slope 3.4% precipitation change per kelvin (much less than the 6.5% per kelvin implied by the Clausius–Clapeyron relation⁴⁴) and intersecting the temperature axis around 1.4 K. Why?

The explanation for these model results is that changes in the overall intensity of the hydrologic cycle are controlled not by the availability of moisture, but by the availability of energy^{44,47}: specifically, the ability of the troposphere to radiate away latent heat released by precipitation. At the simplest level, the energy budgets of the surface and troposphere can be summed up as a net radiative heating of the surface (from solar radiation, partly offset by radiative cooling) and a net radiative cooling of the troposphere to the surface and to space (R) being balanced by an upward latent heat flux (LP , where L is the latent heat of evaporation and P is global-mean precipitation): evaporation cools the surface and precipitation heats the troposphere.

We can approximate the perturbation energy budget of the troposphere as⁴⁷

$$\Delta R_c + \Delta R_t = L\Delta P \quad (1)$$

separating the perturbation radiative cooling, ΔR , into a component, ΔR_c , that is independent of ΔT and a component, ΔR_t , that depends on ΔT . The perturbation latent heating, $L\Delta P$, is about 1 W m^{-2} for a 1% increase in global precipitation. ΔR_c is the change in R that is due directly to external drivers of climate change (that is, change in R that is not mediated via the temperature response to these drivers, and hence approximately independent of ΔT). For example, doubling CO_2 decreases net outgoing infrared radiation through the tropopause (top of the troposphere) by $3\text{--}4 \text{ W m}^{-2}$ (depending on the details of stratospheric adjustment⁴), but also increases downward infrared flux at the surface by about 1 W m^{-2} (ref. 47), giving a negative ΔR_c of -2 to -3 W m^{-2} . In the absence of any significant change in tropospheric temperatures, therefore, increasing CO_2 concentrations reduce the intensity of the hydrologic cycle, an effect observed in early modelling experiments using prescribed sea surface

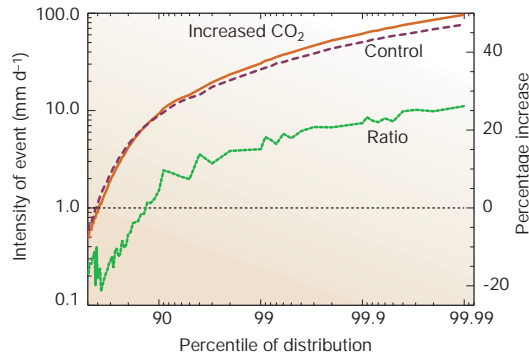


Figure 4 Log–log plot of the distribution of an AOGCM's daily precipitation and how it changes around the time of CO₂ doubling (J. M. Gregory, personal communication). Distribution of daily precipitation (all locations and seasons included) in years 2070–2100 of a transient climate-change simulation⁹⁵ (red) and in the corresponding control simulation (purple). Their ratio is shown by the green curve and right-hand (linear) axis. The global-mean warming is 3.6 K and the tropical mean 3.3 K, giving a Clausius–Clapeyron limit on this ratio of about 22%.

temperatures⁴⁸ (prescribing surface temperatures introduces an infinite heat sink at the surface, but the energy budget of the troposphere still has to balance).

The enhanced radiative cooling due to tropospheric warming, ΔR_T , is approximately proportional to ΔT : tropospheric temperatures scale with the surface temperature change and warmer air radiates more energy, so $\Delta R_T = k_T \Delta T$, with $k_T \approx 3 \text{ W m}^{-2} \text{ K}^{-1}$ (ref. 47). Changes in sensible heat flux at the surface are relatively small and the net effect of water vapour changes on k_T is small assuming (as discussed above) only small changes in the vertical profile of relative humidity⁴⁷. Contributions from clouds vary considerably between models³⁴ and presumably provide the main source of scatter in the relationship of ΔT versus ΔP shown in Fig. 2.

Both ΔR_C and ΔR_T are determined largely by basic features of the radiative and (in the case of ΔR_T) thermal response. Broad features of the pattern of warming, including a reduced equator–pole surface temperature gradient and reduced tropical ‘lapse rate’ (decrease of temperature with height) are much more consistent across climate models than the overall predicted magnitude of the change. Hence both ΔR_C and k_T are much less model-dependent and thus more reliable than is either ΔT or ΔP individually (another potentially useful emergent constraint). This simple picture can explain the main features of the equilibrium responses shown in Fig. 2, including a slope much less than that implied by the Clausius–Clapeyron relation and the line not intersecting the origin. It also has some interesting implications. The 10–90% range in equilibrium warming on doubling CO₂ that is consistent with recent large-scale warming is 1.8–6.5 K (ref. 19), based on the analysis behind Fig. 1. Translating this into a range in the equilibrium precipitation response using the best-fit line shown in Fig. 2 gives a 10–90% range of 0.6–18% (accounting for the scatter of points about the best-fit line, but ignoring uncertainty in the estimated slope, which would make the range slightly larger). Hence we cannot rule out, at even the 10% level, precipitation changes either above or below all currently available model predictions. As for the temperature response, the spread of available AOGCMs underestimates the only available objective estimates of uncertainty in future precipitation change.

Transient global-mean precipitation changes

A further consequence of equation (1) is that the expected precipitation change per degree of global warming, $\Delta P/\Delta T$, depends on the nature of the forcing. In a change driven by short-wave heating at the surface (for example, resulting from solar variability or scattering

aerosols), ΔR_C is small and $\Delta P/\Delta T$ is likely to be larger than in a CO₂-induced change. This effect is illustrated in Fig. 3 where observed global-mean temperature (Fig. 3a) and observed terrestrial precipitation (Fig. 3b) are compared over the past 55 years with the corresponding quantities diagnosed from an ensemble of four simulations using the Met Office's HadCM3 climate model forced with a combination of estimated anthropogenic and natural forcing⁴⁹.

Ensemble members and observations seem to move together, suggesting that both global-mean temperature⁴⁹ and, to a surprising extent, also continental-mean precipitation seem to be controlled by the external forcing. The correlation between the observed (5-year smoothed) precipitation time-series and the ensemble mean over this period is 0.55. This is greater than any correlation found in 98% of cases if we replace the observations with a similar-length, similarly sampled and smoothed segment of the HadCM3 control integration. Hence we can claim to have detected, in the simplest possible sense^{50–52}, the influence of external forcing on global-mean land precipitation.

It is, however, clear that terrestrial precipitation is not simply following the global temperature response. Precipitation changes seem to be dominated by the natural (solar and volcanic) forcing, which varies on shorter timescales, whereas the temperature response is dominated by the anthropogenic forcing, which increases comparatively steadily over this period. This is to be expected, as CO₂ is less effective in driving changes in global precipitation than is short-wave forcing of a similar magnitude because, in the former case, ΔR_C and ΔR_T in equation (1) tend to cancel each other out. Of course, both forcings could alter the distribution of precipitation between land and sea: we would prefer to compare global precipitation changes, but the necessary long-term data sets are not available³⁸.

Thus, although there is clearly usable information in Fig. 3, it would be physically unjustified to estimate $\Delta P/\Delta T$ directly from twentieth-century observations and assume that the same quantity will apply in the future, when the balance between climate drivers will be very different³³. Likewise, the approach of ref. 18 (estimating the size of the anthropogenic change from the observed record and using this to recalibrate anthropogenic changes simulated by climate models), although applicable in principle to precipitation, is unlikely to be useful at present. This is because the anthropogenic contribution to precipitation changes during the twentieth century is still weak compared with natural fluctuations (both unforced and externally driven). How, therefore, can we set about constraining the future transient response of the hydrologic cycle to anthropogenic forcing?

The transient responses of the CMIP-2 experiments, shown by the green diamonds in Fig. 2, seem to cluster above the distribution of equilibrium responses in the ΔT versus ΔP plane. Although the basic tropospheric energy budget displayed in equation (1) still applies, the relationship between ΔR_T and ΔT seems to be slightly different in the transient case. This discrepancy is probably due, at least in part, to systematic differences between transient and equilibrium patterns of warming: in particular, land areas tend to warm faster than oceans in transient experiments in all models. To first order, we might expect the discrepancy to be proportional to the net heat flux into the oceans in the transient experiments, F_s , which is a measure of the extent to which these experiments are out of equilibrium. Hence the tropospheric energy budget for a CMIP-2 scenario can be written

$$\Delta R_C + k_T \Delta T - \kappa F_s = \Delta P \quad (2)$$

with ΔR_C and k_T taking values appropriate to the equilibrium response experiments and the empirical constant κ being estimated from the CMIP-2 results. The relationship between ΔP and ΔT in the CMIP-2 results is too weak either to confirm equation (2) or to constrain κ effectively, so we are simply proposing this as a plausible

Box 1

Towards objective probabilistic climate forecasting

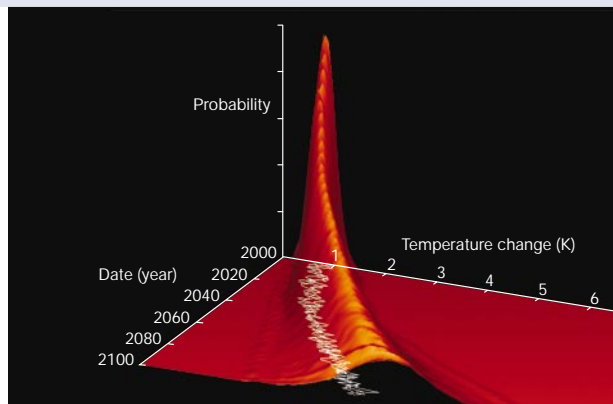
Myles R. Allen & David A. Stainforth

A climate forecast is intrinsically five-dimensional, spanning space, time and probability. Mainstream climate modelling has, so far, sacrificed probabilistic resolution almost completely in favour of the other four dimensions¹. Correcting this imbalance requires a new approach. Hitherto, forecasts have explored uncertainty in initial conditions²⁻³ (see Box 1 Figure opposite) as well as the impact of altering boundary conditions, such as adopting different scenarios of future concentrations of greenhouse gases⁴. For many variables, however, the main uncertainty in multi-decade climate prediction is not in the initial state nor in the external driving, but in the climate system's response⁵. Where this issue has been addressed with atmosphere-ocean general circulation models (AOGCMs) it is primarily through unconstrained 'ensembles of opportunity' based on comparisons between different models with no direct reference to observations^{4,6}. These, we have argued, are likely to provide a misleadingly small (over-optimistic) impression of forecast uncertainty⁷.

At the most basic level, the community needs to agree on what is meant by a 'correct' estimate of risk in climate forecasting. A probabilistic climate forecast (for example, of the risk of global precipitation increasing by more than 10% by 2050) cannot be checked against observations as can a probabilistic weather forecast. If a two-day weather forecast is wrong at the 5% level much more than 5% of the time, then something is amiss with the forecasting system. If a 50-year climate forecast is 'wrong' at the 5% level, we could simply have been unlucky. This apparent difficulty with verification has led to the view that estimates of uncertainty based on expert opinion (for example, the range for climate sensitivities used by ref. 8) are as good as any other⁹. This leaves the field open to the charge of subjectivism.

Objectively, we need to ask: 'given the observations available now, what range of forecasts might we have obtained had we started again from scratch many times over and made completely independent sets of decisions about model formulation and resolution?' A probabilistic forecast can only be said to have converged when including additional models is unlikely to make much difference to the forecast distribution of a particular variable. But there are complications. For example, we have no way of defining how 'close' two models are solely in terms of their formulation⁷, so we cannot design a representative sampling strategy over 'all possible AOGCMs' even if we had the resources to do so. In practice, therefore, a probabilistic forecast must begin with a very large ensemble of possible models, obtained by varying parameter values, parameterization schemes, resolution and entire model components, and extracting a sub-sample weighted according to the different models' ability to simulate recent observed climate change. A probabilistic forecast based on this sub-sample will have converged if its spread is determined primarily by the constraint of consistency with observations and not by the choice of models within the original ensemble — this is the crucial distinction between a constrained ensemble and an unconstrained ensemble of opportunity.

For some variables, probabilistic forecasts may be converging already. Given the emergent constraints relating past to future greenhouse warming that seem to hold across all available climate models, the distribution of forecast global-mean temperature changes in Fig. 1 is determined not by the choice of model(s), but by uncertainty in how much recent warming can be attributed to CO₂ increase. This uncertainty is due primarily to other signals and internal variability in the observed climate record. It will reduce as the signal strengthens⁵, but it may not change much as models improve. We would argue that this is both more robust (less subject to short-term revision) and more reliable (acceptable to non-specialists as a basis for action) than a forecast based on expert opinion.



Box 1 Figure The three-dimensional surface shows a forecast probability distribution of a one-dimensional quantity (global-mean warming above pre-industrial), accounting for uncertainty in the climate response, while the lines show the (smaller) impact of initial condition uncertainty in an ensemble of model simulations. Data courtesy of P. Stott (Met Office) and J. Kettleborough (Rutherford Appleton Laboratory)⁵, based on the IPCC SRES A2 scenario.

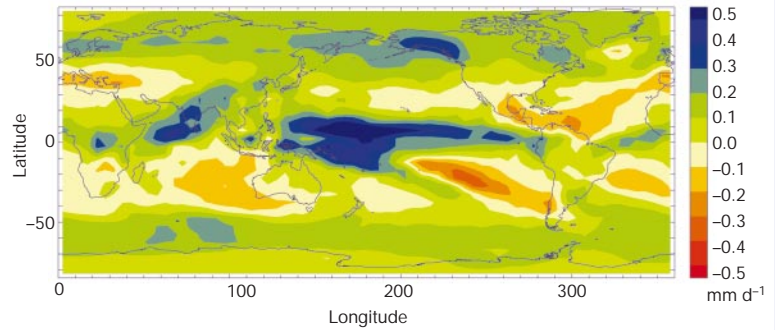
When will we be able to say that forecast changes in the hydrologic cycle have converged enough to be trusted? We made a tentative estimate of the distribution of global-mean precipitation change in Fig. 2, primarily to show that distributions based only on the spread of current AOGCMs should not be trusted. To extend this to regional changes, we need to repeat the analysis behind Fig. 1 with a full-scale AOGCM. Figure 1 required many hundreds of integrations to explore just three uncertain parameters in a two-dimensional climate model¹⁰, and there are hundreds of such uncertainties in an AOGCM. The chaotic nature of an AOGCM means that many of the techniques used in shorter-range forecasting to select perturbations¹¹ are not directly applicable to the climate problem¹²; it also means that several simulations will be needed to assess the impact of every perturbation to the model's formulation.

Thus, objective probabilistic forecasts of regional changes in rainfall and other climate variables will require numbers of simulations several orders of magnitude larger than the CMIP-2 experiment, the largest ensemble of AOGCM simulations undertaken to date. New approaches utilizing distributed computing and the emerging electronic 'grid' may provide a way forward^{13,14}, and readers interested in participating in such an initiative¹⁵ may wish to contact us on <http://www.climateprediction.net>.

Dave Stainforth is at Atmospheric, Oceanic and Planetary Physics, Department of Physics, University of Oxford, Clarendon Laboratory, Parks Road, Oxford OX1 3PU, UK (e-mail: d.stainforth1@physics.ox.ac.uk)

- Schneider, S. H. *Nature* **411**, 17–19 (2001).
- Mitchell, J. F. B., Johns, T. C., Gregory, J. M. & Tett, S. F. B. *Nature* **376**, 501–504 (1995).
- Dai, A., Meehl, G. A., Washington, W. M., Wigley, T. M. L. & Arblaster, J. M. *Bull. Am. Meteorol. Soc.* **82**, 2377–2388 (2001).
- Cubasch, U. *et al.* in *Climate Change 2001, The Science of Climate Change* Ch. 9 (eds Houghton, J. T. *et al.*) 527–582 (Cambridge Univ. Press, Cambridge, 2001).
- Stott, P. A. & Kettleborough, J. A. *Nature* **416**, 723–726 (2002).
- Palmer, T. N. & Raisanen, J. *Nature* **415**, 512–514 (2002).
- Smith, L. A. *Proc. Natl Acad. Sci. USA* **99**, 2487–2492 (2002).
- Wigley, T. M. L. & Raper, S. C. B. *Science* **293**, 451–454 (2001).
- Giles, J. *Nature* **418**, 476–478 (2002).
- Forest, C. E. *et al.* *Science* **295**, 113–117 (2002).
- Palmer, T. N. *Rep. Prog. Phys.* **63**, 71–116 (2000).
- Lea, D. J., Allen, M. R. & Haine, T. W. N. *Tellus* **52A**, 523–532 (2000).
- Hansen, J. A., Allen, M. R., Stainforth, D. A., Heaps, A. & Stott, P. A. *World Resource Rev.* **13**, 187–189 (2001).
- Stainforth, D. A. *et al.* *Comput. Sci. Eng.* **4**, 82–89 (2002).
- Allen, M. R. *Nature* **401**, 642 (1999).

Figure 5 Precipitation change at the time of CO₂ doubling averaged over all the members of the CMIP-2 ensemble for which the data were available (14 models), for the 20 years centred on the time of CO₂ doubling.



correction for disequilibrium. The scatter of CMIP-2 results is consistent with what we would expect from the equilibrium response experiments. Thus, the problem is not too much noise, but too little signal — we do not have a wide enough range of ΔT or ΔP from the transient experiments to identify the relationship between them (see Box 1).

Drawing this evidence together, we can infer a distribution for ΔP at the time of CO₂ doubling under a scenario of an annual 1% increase in CO₂ concentration from the distribution of ΔT shown in Fig. 1 (the green dashed curve in Fig. 2) augmented with κF_s (blue dashed curve in Fig. 2, with the distribution of F_s estimated using the same analysis that yields Fig. 1; ref. 19). We translate this into a distribution for ΔP (red dashed curve in Fig. 2) using the best-fit line through the equilibrium response experiments, including additional variance to account for the scatter. It must be emphasized that these distributions use information on TCR and climate sensitivity only as constrained by observations of recent changes in temperature and ocean heat content. They do not depend on precipitation changes in the intermediate-complexity model used to derive the distribution function in Fig. 1 (which are likely to be model specific⁵⁴), nor do they make use of observed precipitation changes. It may seem counter-intuitive to use temperature and ocean heat content rather than precipitation observations to constrain future precipitation, but with global precipitation controlled by energetic constraints, and with the precipitation response to anthropogenic forcing being difficult to disentangle from other signals in the observations, this could be the best strategy available.

The precise distributions shown on Fig. 2 naturally depend on details of the analysis, but the key conclusion is that the current range of uncertainty in ΔP is considerably larger than the spread of current model responses. This analysis suggests a 25% chance of $\Delta P > 5\%$, the highest response of the coupled models shown in Fig. 2, and a 15% chance of $\Delta P > 6\%$, the response of the ‘outlier’ model mentioned above⁴ (for which the data needed for Fig. 2 are unavailable). The upper 5th percentile, often used in decision-making as a standard upper bound, could exceed the highest ΔP observed in current models by over 50%. The message is clear: impact assessments that rely on intermodel spread⁵⁵ could seriously underestimate the range of uncertainty in precipitation change in the twenty-first century.

A similar analysis could easily be extended to any variable that shows a simple functional relationship across a wide variety of models to quantities that are constrained by current observations, such as global temperatures and rates of ocean heat uptake over the coming decades. Of course there are caveats. In particular, the limited diversity of available slab and coupled AOGCMs makes it difficult to establish whether any relationship (such as the straight line in Fig. 2) has converged or is simply an artefact of resolution or sampling. Moreover, the use of an intermediate-complexity model to derive the forecast temperature distribution may underestimate the complexity of responses that are consistent with recent observations. Both of these caveats mean the spread of the forecast distribution of precipitation change is likely to be underestimated, so that the problems

with using inter-model spread would be even worse than suggested by the comparisons above. Both caveats could be substantially resolved with the use of much larger, systematically perturbed ensemble forecasts with AOGCMs (see Box 1).

Changes in precipitation extremes

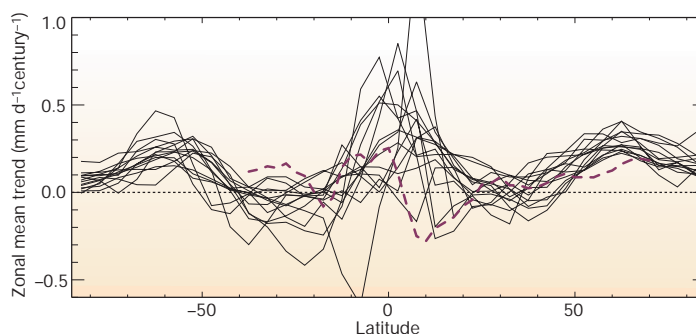
Long-term mean precipitation is a useful summary indicator of the intensity of the hydrologic cycle, but details of the distribution of precipitation over time, including the peak intensity of precipitation events and duration of prolonged droughts, are likely to be the most important issues in determining impacts of precipitation changes⁹. Although global-mean precipitation is primarily constrained by the energy budget, the heaviest rainfall events are likely to occur when effectively all the moisture in a volume of air is precipitated out, suggesting that the intensity of these events will increase with the availability of moisture⁷ (that is, significantly faster than the global mean). Thus we might expect the uppermost quantiles of the rainfall distribution to increase by about 6.5% per kelvin (ref. 44) if the ambient flows change (most likely at higher latitudes). In the tropics, where the flows leading to precipitation are themselves driven largely by the latent heat released by precipitation, larger increases still might occur⁷. In particular, the maximum thermodynamically possible rainfall and winds in hurricanes are predicted to increase rapidly with warming⁵⁶.

The red and purple curves in Fig. 4 show the magnitude of daily precipitation as a function of percentile of the precipitation distribution in one AOGCM under climate change and control conditions, respectively. The green curve (and right-hand axis) shows the ratio between them. At the highest end of the distribution (all tropical cases), it appears to be converging to about a 25% increase, which is indeed slightly more than we would expect from the Clausius–Clapeyron relationship.

Because such increases are more than double the increase in global-mean precipitation (that is, the change summed over all percentiles, which is constrained by the energy budget, not by the Clausius–Clapeyron relation), there must be decreases lower down the distribution. Indeed, the increase at the heaviest rain events is large enough that the energy constraint on the total implies that only on one day in ten does precipitation increase (the control and perturbed distributions cross around the 90th percentile in Fig. 4). It would be interesting to know how other models compare — if this were another emergent constraint generic over all models in regions of interest, then we could use forecast temperature changes to constrain extreme as well as mean precipitation. Given the acknowledged difficulties in relying on model simulations of extreme events and in observing changes in extremes directly⁵⁷, this could be a powerful result. In particular, this convergence to a particular fractional increase, possibly related to the Clausius–Clapeyron limit, could even improve as we move to the highest percentiles, which are generally the least tractable under more direct approaches.

Even modest increases in the magnitude of events in the tails of the distribution can have a very substantial impact on the expected

Figure 6 Zonal-mean precipitation trends over the 70 years to CO₂ doubling in the CMIP-2 ensemble and observed trends in terrestrial precipitation over the past century. Each thin solid line is for a member of the CMIP-2 ensemble (forced with CO₂ changes alone), whereas the thick dashed line is the observed trend over the twentieth century from land-based observations.



return times of events of a given magnitude^{8–10,58}. Such changes may already be occurring^{59,60}: the model used by ref. 61 suggested that, over the United Kingdom, floods of the magnitude expected to occur every 20 years in 1860 might now be expected every 5 years. Figure 4 implies that the corresponding changes might be even more significant in tropical regions¹⁰.

Regional precipitation

Although the large-scale temperature response to climate-change forcings is predicted to be relatively smooth (usually with the same sign everywhere), precipitation varies much more in space and time and is notoriously much harder to simulate correctly in models. It is no surprise then that predicted changes in local precipitation vary considerably both in space and between models. Figure 5 shows the CMIP-2 ensemble-mean pattern of regional precipitation change around the time of CO₂ doubling, while Fig. 6 shows the zonal-mean changes in each model.

The ensemble-mean precipitation change conceals a wide variety of responses across the CMIP-2 ensemble. Only 30% of the variance between models of predicted precipitation changes on a 5° × 5° grid is accounted for by a single common response pattern, compared to over 90% for temperature. The standard deviation between the various models' predictions is greater than the mean response shown in Fig. 5 everywhere between 50° N and 50° S apart from a small region in the equatorial West Pacific. The natural assumption that there can then be no useful information there may be over-pessimistic, as the small scales of precipitation variation tend to mask a closer agreement in physical terms. For example, if some set of models all shifted a particular rainband in the same direction, but its position varied between their base climates by as much as its width, one would see completely inconsistent results at a single point.

The zonal-mean response (Fig. 6) is more coherent across models, with strong increase in precipitation near the Equator, some reduction in sub-tropical subsidence regions and a smaller but more consistent increase in mid-latitudes. In short, the general tendency is for precipitation to increase in regions where it is high and decrease where evaporation is high, which is just what one might expect from the increased specific humidities leading to increased atmospheric fluxes of humidity from its sources to its sinks⁶². One consequence of this is that mid-continental summer droughts may become more frequent and intense⁶³, a common feature of model simulations of greenhouse warming^{64,65}. In interpreting any such features, however, it must be emphasized that imperfections in AOGCMs affect precipitation more than many other fields of general interest. For example, AOGCMs generally do not allow for the time convection takes to develop and hence simulate incorrectly the timing of precipitation over the course of a day. This can have knock-on effects on total precipitation.

The pattern of change shows a 'horseshoe' pattern reminiscent of the El Niño/Southern Oscillation (ENSO) phenomenon. Hence the interpretation of any trend is closely related to the question of whether the apparent⁶⁶, albeit debatable^{67,68}, increase in the frequency

and intensity of ENSO events over the past few decades is genuine and, if so, anthropogenic^{69,70}.

Figure 6 also shows the zonal-mean 100-year trend in observed precipitation from the Hulme dataset of land-based station observations^{38,71}. We see an increase in southern equatorial regions and in mid-latitudes, broadly consistent with the models and our physical expectations⁵³. But this is only a qualitative comparison, given that the land-based data sample less than a third of the world, the strongest precipitation changes in Fig. 5 seem to be occurring over the oceans, the forcing over the twentieth century is very different from the CMIP-2 experiments, and different forcings may well be associated with different patterns of response. Anthropogenic aerosols, in particular, are so geographically concentrated that circulation changes and other local effects might swamp the driving mechanism outlined above. Additionally, aerosols might affect precipitation more directly through their impact on cloud microphysics (ref. 5, and see review in this issue by Kaufman *et al.*, pages 215–223). Nevertheless, the apparent robustness of the basic features and agreement with a simple physical explanation are encouraging.

Because land-based precipitation records may miss most of the signal (Fig. 5), the advent of global satellite-derived precipitation analyses^{72–76} is welcome. Apparently significant positive trends in tropical precipitation and the strength of the Hadley circulation (the zonal-mean flow at low latitudes, fuelled by latent heat release) have been reported^{77,78}, although issues over decadal variability and the long-term stability of observationally based data sets remain^{79,80}.

An important factor for the regional details of the precipitation response to external forcing is the change in atmospheric circulation^{6,81}. In particular, an intensification of the North Atlantic Oscillation — more westerly winds across the North Atlantic and into Eurasia — has been observed over the past few decades^{81,82}. Although models (and simple theory) indicate that such a change, which would increase mid-latitude land precipitation, might be expected to accompany an anthropogenic greenhouse warming⁸³, most models seem to underestimate the magnitude of this circulation change⁸⁴. Extra-tropical circulation and precipitation anomalies may well be strongly influenced by driving from the tropics (refs 85, 86, and M. Blackburn and B. Hoskins, personal communication), and it remains very doubtful whether current AOGCMs respond correctly to localized but remote forcing^{83,87}.

Interactions with aerosols and oceans

We have concentrated above on the effects of CO₂, the largest single driver of temperature changes over the twentieth century and expected to be the dominant one in the twenty-first century⁸⁸. But aerosols also seem to have contributed significantly to recent large-scale temperature changes^{49,50} and may have had important effects locally. The most important overall are thought to be sulphate aerosols from volcanic and anthropogenic sources in the stratosphere and troposphere, respectively. Their primary radiative effect is to increase the scattering of sunlight away to space, either directly or in the case of the troposphere via (very uncertain) effects on clouds (refs 5, 88, and see

review in this issue by Kaufman *et al.*, pages 215–223). Thus, their primary effect is to provide a surface cooling and so a greater precipitation response compared to changes in CO₂ concentrations.

Aerosols can also produce direct tropospheric heating (refs 5, 88, and review by Kaufman), with similar effects to CO₂ on the hydrologic cycle. The effects of warming on the atmospheric moisture content, maximum rainfall amounts and the zonal-mean precipitation discussed above should all apply regardless of the cause of the warming. Aerosol-driven changes in precipitation efficiency could in principle disturb the energy-balance arguments by changing the sensible heat flux between surface and troposphere. It should be noted, however, that calculating the forcing due to well-mixed greenhouse gases, with well-defined spectral properties that can be measured in the laboratory, is much easier than the forcing due to the many possible types of aerosol, with their shorter lifetimes and complex distribution, so here we must expect rather more modelling uncertainty.

A potentially important effect of precipitation changes is on the thermohaline circulation (THC) of the North Atlantic³⁴. This brings warm water northward to give an important warming of northern mid-latitudes (refs 13, 89, and see review in this issue by Rahmstorf, pages 207–214). The apparently robust increase in high-latitude rainfall discussed above would tend to weaken the THC by stabilizing the oceanic water column in regions of deep convection (refs 13, 14, 90, and the review by Rahmstorf). The possibility has even been raised of a complete and long-term collapse in the THC, which would have a major impact on European climate in particular. Most climate models show some weakening of the THC under greenhouse-gas-induced warming, but the amount of weakening is model-dependent^{14,91}, and no constraint analogous to that shown in Fig. 2 has yet been found when comparing different models. Hence we cannot yet quantify the chance of a THC collapse during the twenty-first century.

Underestimated uncertainties

The climate modelling community has, for lack of any alternative, long used the spread of results from their AOGCMs as a subjective indicator of the range of uncertainty in climate forecasts. Modellers have, however, always understood that this range does not provide a meaningful confidence interval, as each model is designed largely as a 'best guess' and modellers share views, data, algorithms and hence, inevitably, errors⁹². The spread of results from such an 'ensemble of opportunity' is therefore likely to underestimate the true range of uncertainty in a climate forecast.

In the absence of objective probabilistic forecasts with numerical models that systematically investigate the range of possible responses of the hydrologic cycle to anthropogenic climate change^{93,94}, we have here attempted to constrain the expected changes by other means. We have, nominally, detected the influence of external forcing on recent terrestrial precipitation changes, but isolating the anthropogenic contribution is difficult as observed large-scale changes in precipitation — unlike temperature — seem to be dominated by natural forcing. Hence we cannot constrain future precipitation directly with recent precipitation trends.

Alternatively, we combine an observationally constrained estimate of 1.8–6.5 K for the 10–90% range in equilibrium warming on doubling CO₂ with a precipitation increase of 3.4% per °C of warming (plus an offset and some scatter) as obtained from a number of coupled models with idealized oceans. This gives a corresponding range for the equilibrium precipitation response of 0.6–18%. This exceeds the range of simulations of the precipitation response given by current 'best guess' climate models.

Precipitation changes predicted from climate models depend heavily on the simulations of present-day precipitation, which have many deficiencies. Hence we will continue to need conventional model development, including additional processes and exploring the impact of higher resolution. But we should not sacrifice everything on the altar of spatial resolution: ultra-high-resolution models

are too expensive to be used systematically to identify the constraints (linking observable to predicted climate variables) that are essential to probabilistic climate forecasting. We believe (see Box 1) that objective probabilistic forecasting using AOGCMs is now possible, and that it is worth rising to the challenge. A forecasting system that rules out some currently conceivable futures as unlikely could be far more useful for long-range planning than a small number of ultra-high-resolution forecasts that simply rule in some (very detailed) futures as possibilities. □

doi:10.1038/nature01092

- Palmer, T. N. Predicting uncertainty in forecasts of weather and climate. *Rep. Prog. Phys.* **63**, 71–116 (2000).
- Smith, L. A. What might we learn from climate forecasts? *Proc. Natl Acad. Sci. USA* **99**, 2487–2492 (2002).
- Folland, C. K. *et al.* in *Climate Change 2001, The Science of Climate Change* Ch. 2 (eds Houghton, J. T. *et al.*) 101–181 (Cambridge Univ. Press, Cambridge, 2001).
- Cubasch, U. *et al.* in *Climate Change 2001, The Science of Climate Change* Ch. 9 (eds Houghton, J. T. *et al.*) 527–582 (Cambridge Univ. Press, Cambridge, 2001).
- Ramanathan, V., Crutzen, P. J., Kiehl, J. T. & Rosenfeld, D. Atmosphere—aerosols, climate and the hydrological cycle. *Science* **294**, 2119–2124 (2001).
- Carnell, R. E. & Senior, C. A. Changes in mid latitude variability due to increasing greenhouse gases and sulphate aerosols. *Clim. Dynam.* **14**, 369–383 (1998).
- Trenberth, K. E. Conceptual framework for changes of extremes of the hydrological cycle with climate change. *Clim. Change* **42**, 327–339 (1999).
- Kharin, V. V. & Zwiers, F. W. Changes in the extremes in an ensemble of transient climate simulations with a coupled atmosphere-ocean GCM. *J. Clim.* **13**, 3760–3788 (2000).
- Meehl, G. A. *et al.* Trends in extreme weather and climate events: issues related to modelling extremes in projections of future climate change. *Bull. Am. Meteorol. Soc.* **81**, 427–436 (2000).
- Palmer, T. N. & Räisänen, J. Quantifying the risk of extreme seasonal precipitation events in a changing climate. *Nature* **415**, 512–514 (2002).
- Osborn, T. J., Hulme, M., Jones, P. D. & Basnett, T. A. Observed trends in the daily intensity of United Kingdom precipitation. *Int. J. Climatol.* **20**, 347–364 (2000).
- Milly, P. C. D., Wetherald, R. T., Dunne, K. A. & Delworth, T. L. Increasing risk of great floods in a changing climate. *Nature* **415**, 514–517 (2002).
- Rahmstorf, S. Bifurcations of the Atlantic thermohaline circulation in response to changes in the hydrological cycle. *Nature* **378**, 145–149 (1995).
- Clark, P. U., Pisias, N. G., Stocker, T. F. & Weaver, A. J. The role of the thermohaline circulation in abrupt climate change. *Nature* **415**, 863–869 (2002).
- Pierrehumbert, R. T. in *Mechanisms of Global Climate Change at Millennial Time Scales* (Geophys. Monogr. 112) 339–361 (American Geophysical Union, Washington DC, 1999).
- Andronova, N. G. & Schlesinger, M. E. Causes of global temperature changes during the 19th and 20th centuries. *Geophys. Res. Lett.* **27**, 2137–2140 (2000).
- Forest, C. E., Allen, M. R., Stone, P. H. & Sokolov, A. P. Constraining uncertainties in climate models using climate change detection techniques. *Geophys. Res. Lett.* **27**, 569–572 (2000).
- Allen, M. R., Stott, P. A., Mitchell, J. F. B., Schnur, R. & Delworth, T. Quantifying the uncertainty in forecasts of anthropogenic climate change. *Nature* **407**, 617–620 (2000).
- Forest, C. E., Stone, P. H., Sokolov, A. P., Allen, M. R. & Webster, M. D. Quantifying uncertainties in climate system properties with the use of recent climate observations. *Science* **295**, 113–117 (2002).
- Gregory, J. M., Stouffer, R., Raper, S., Rayner, N. & Stott, P. A. An observationally-based estimate of the climate sensitivity. *J. Clim.* (in the press).
- Allen, M. R. Do-it-yourself climate prediction. *Nature* **401**, 642 (1999).
- Wigley, T. M. L. & Raper, S. C. B. in *Climate and Sea Level Change: Observations, Projections and Implications* (eds Warrick, R. A., Barrow, E. M. & Wigley, T. M. L.) Ch. 7 (Cambridge Univ. Press, Cambridge, 1993).
- Sokolov, A. P. & Stone, P. H. A flexible climate model for use in integrated assessments. *Clim. Dynam.* **14**, 291–303 (1998).
- Meehl, G. A., Boer, G. J., Covey, C., Latif, M. & Stouffer, R. J. The Coupled Model Intercomparison Project (CMIP). *Bull. Am. Meteorol. Soc.* **81**, 313–318 (2000).
- Covey, C., AchutaRao, K. M., Lambert, S. J. & Taylor, K. E. Intercomparison of present and future climates simulated by coupled ocean-atmosphere GCMs. Tech. Rep. 66 (Program for Climate Model Diagnosis and Intercomparison, Livermore, 2000).
- Cubasch, U. *et al.* Monte Carlo climate change forecasts with a global coupled ocean-atmosphere model. *Clim. Dynam.* **10**, 1–19 (1994).
- Levitus, S., Antonov, I. I., Boyer, T. P. & Stephens, C. Warming of the world ocean. *Science* **287**, 2225–2229 (2000).
- Barnett, T. P., Pierce, D. W. & Schnur, R. Detection of anthropogenic climate change in the world's oceans. *Science* **292**, 270–274 (2001).
- Stott, P. A. & Kettleborough, J. A. Origins and estimates of uncertainty in predictions of twenty-first century temperature rise. *Nature* **416**, 723–726 (2002).
- Knutti, R., Stocker, T. F., Joos, F. & Plattner, G. K. Constraints on radiative forcing and future climate change from observations and climate model ensembles. *Nature* **416**, 719–723 (2002).
- Webster, M. D. *et al.* Uncertainty analysis of global climate change projections. Tech. Rep. 73 <http://web.mit.edu/globalchange/www/rpt73.html> (Massachusetts Institute of Technology, Cambridge, MA, 2001).
- Nozawa, T., Emori, S., Nakajima, A., Takemura, T. & Numaguti, A. in *Present and Future of Modelling Global Environmental Change: Towards Integrated Modelling* (ed. Matsuno, T.) (Terra Scientific, Tokyo, 2001).
- Arrhenius, S. On the influence of carbonic acid in the air upon the temperature of the ground. *Phil. Mag. Ser. 5*, **41**, 237–276 (1896).
- Stocker, T. F. *et al.* in *Climate Change 2001: The Scientific Basis* Ch. 7 (eds Houghton, J. T. *et al.*) 417–470 (Cambridge Univ. Press, Cambridge, 2001).

35. Ingram, W. J. On the robustness of the water vapor feedback: GCM vertical resolution and formulation. *J. Clim.* **15**, 917–921 (2002).
36. Schoneweise, C. D. & Rapp, J. *Climatic Trends Atlas of Europe Based on Observations 1891–1990* (Kluwer, 1997).
37. Gaffen, D. J., Rosen, R. D., Salstein, D. A. & Boyle, J. S. Evaluation of tropospheric water vapor simulations from the atmospheric model intercomparison project. *J. Clim.* **10**, 1648–1661 (1999).
38. New, M., Hulme, M. & Jones, P. Representing twentieth-century space-time climate variability. part ii: Development of 1901–96 monthly grids of terrestrial surface climate. *J. Clim.* **13**, 2217–2238 (2000).
39. Ross, R. J., Elliott, W. P. & Seidel, D. J. Lower-tropospheric humidity-temperature relationships in radiosonde observations and atmospheric general circulation models. *J. Hydrometeorol.* **3**, 26–38 (2001).
40. Zhai, P. M. & Eskridge, R. E. Atmospheric water vapor over china. *J. Clim.* **10**, 2643–2652 (1997).
41. Elliott, W. P. On detecting long-term changes in atmospheric moisture. *Clim. Change* **31**, 349–367 (1995).
42. Bates, J. J., Jackson, D. L., Breon, F. M. & Bergen, Z. D. Variability of tropical upper tropospheric humidity 1979–1998. *J. Geophys. Res.* **106**, 32271–32281 (2001).
43. Soden, B. J., Wetherald, R. T., Stenchikov, G. L. & Robock, A. Global cooling after the eruption of Mount Pinatubo: a test of climate feedback by water vapor. *Science* **296**, 727–730 (2002).
44. Boer, G. J. Climate change and the regulation of the surface moisture and energy budgets. *Clim. Dynam.* **8**, 225–239 (1993).
45. LeTreut, H. & McAvaney, B. J. A model intercomparison of equilibrium climate change in response to CO₂ doubling. Tech. Rep. 18 (Institute Pierre Simon LaPlace, Paris, 2000).
46. Schlesinger, M. E. & Mitchell, J. F. B. in *Projecting the Climatic Effects of Increasing Carbon Dioxide* (eds MacCracken, M. C. & Luther, F. M.) 81–147 (United States Dept Energy, 1985).
47. Mitchell, J. F. B., Wilson, C. A. & Cunningham, W. M. On CO₂ climate sensitivity and model dependence of results. *Q. J. R. Meteorol. Soc.* **113**, 293–322 (1987).
48. Mitchell, J. F. B. The seasonal response of a general circulation model to changes in CO₂ and sea temperatures. *Q. J. R. Meteorol. Soc.* **109**, 113–152 (1983).
49. Stott, P. A. *et al.* External control of twentieth century temperature by natural and anthropogenic forcings. *Science* **290**, 2133–2137 (2000).
50. Mitchell, J. F. B. *et al.* in *Climate Change 2001, The Science of Climate Change* Ch. 12 (eds Houghton, J. T. *et al.*) 697–738 (Cambridge Univ. Press, Cambridge, 2001).
51. Santer, B. D. *et al.* A search for human influences on the thermal structure of the atmosphere. *Nature* **382**, 39–46 (1996).
52. Tett, S. F. B., Mitchell, J. F. B., Parker, D. E. & Allen, M. R. Human influence on the atmospheric vertical temperature structure: detection and observations. *Science* **247**, 1170–1173 (1996).
53. Hulme, M., Osborne, T. J. & Johns, T. C. Precipitation sensitivity to global warming: comparison of observations with HadCM2 simulations. *Geophys. Res. Lett.* **25**, 3379–3382 (1998).
54. Sokolov, A., Forest, C. E. & Stone, P. H. A comparison of the behaviour of different AOGCMs in transient climate change experiments. Tech. Rep. 81 (MIT Joint Program on the Science and Policy of Global Change, Cambridge, MA, 2001).
55. Hulme, M., Turnpenny, J. & Jenkins, G. Climate change scenarios for the United Kingdom: the UKCIP Briefing Report (Tyndall Centre for Climate Change Research, 2002).
56. Emanuel, K. A. The dependence of hurricane intensity on climate. *Nature* **326**, 483–485 (1987).
57. Giorgi, F. *et al.* in *Climate Change 2001, The Science of Climate Change* Ch. 10 (eds Houghton, J. T. *et al.*) 585–638 (Cambridge Univ. Press, Cambridge, 2001).
58. Groisman P. Ya *et al.* Changes in the probability of heavy precipitation: important indicators of climatic change. *Clim. Change* **42**, 243–283 (1999).
59. Karl, T. R., Knight, R. W. & Plummer, N. Trends in high-frequency climate variability in the twentieth century. *Nature* **377**, 217–220 (1995).
60. Karl, T. R. & Knight, R. W. Secular trends of precipitation amount, frequency, and intensity in the united states. *Bull. Am. Meteorol. Soc.* **79**, 231–241 (1998).
61. Huntingford, C. *et al.* Regional climate model predictions of extreme rainfall for a changing climate. *Q. J. R. Meteorol. Soc.* (in the press).
62. Manabe, S. & Wetherald, R. T. On the distribution of climate change resulting from an increase in CO₂ content of the atmosphere. *J. Atmos. Sci.* **37**, 99–118 (1980).
63. Dai, A., Trenberth, K. E. & Karl, T. R. Global variations in droughts and wet spells: 1900–1995. *Geophys. Res. Lett.* **25**, 3367–3370 (1998).
64. Gregory, J. M., Mitchell, J. F. B. & Brady, A. J. Summer drought in northern mid-latitudes in a time-dependent CO₂ climate experiment. *J. Clim.* **10**, 662–686 (1997).
65. Wetherald, R. T. & Manabe, S. Detectability of summer dryness caused by greenhouse warming. *Clim. Change* **43**, 495–511 (1999).
66. Trenberth, K. E. & Hoar, T. J. The 1990–1995 El Niño/Southern Oscillation event: the strongest on record? *Geophys. Res. Lett.* **23**, 57–60 (1996).
67. Wunsch, C. The interpretation of short climate records, with comments on the North Atlantic and Southern Oscillations. *Bull. Am. Meteorol. Soc.* **80**, 245–255 (1999).
68. Trenberth, K. E. & Hurrell, J. E. Comments on: ‘The interpretation of short climate records, with comments on the North Atlantic and Southern Oscillations’. *Bull. Am. Meteorol. Soc.* **80**, 2721–2722 (1999).
69. Timmermann, A. *et al.* Increased El Niño frequency in a climate model forced by future greenhouse warming. *Nature* **398**, 694–696 (1999).
70. Collins, M. Understanding uncertainties in the response of ENSO to greenhouse warming. *Geophys. Res. Lett.* **27**, 3509–3513 (2000).
71. Hulme, M. A 1951–80 global land precipitation climatology for the evaluation of general-circulation models. *Clim. Dynam.* **7**, 57–72 (1992).
72. Huffman, G. J. *et al.* The global precipitation climatology project (GPCP) combined precipitation dataset. *Bull. Am. Meteorol. Soc.* **78**, 5–20 (1997).
73. Spencer, R. W. Global oceanic precipitation from the msu during 1979–91 and comparisons to other climatologies. *J. Clim.* **6**, 1301–1326 (1993).
74. Xie, P. P. & Arkin, P. A. Global precipitation: a 17-year monthly analysis based on gauge observations, satellite estimates, and numerical model outputs. *Bull. Am. Meteorol. Soc.* **78**, 2539–2558 (1997).
75. New, M., Todd, M., Hulme, M. & Jones, P. Precipitation measurements and trends in the twentieth century. *Int. J. Clim.* **21**, 1899 (2001).
76. Huffman, G. J. *et al.* Global precipitation at one-degree daily resolution from multisatellite observations. *J. Hydrometeorol.* **2**, 36–50 (2001).
77. Trenberth, K. E. & Caron, J. M. Estimates of meridional atmosphere and ocean heat transports. *J. Clim.* **14**, 3433–3443 (2001).
78. Chen, J. Y., Carlson, B. E. & Del Genio, A. D. Evidence for strengthening of the tropical general circulation in the 1990s. *Science* **295**, 838–841 (2002).
79. Wielicki, B. A. *et al.* Evidence for large decadal variability in the tropical mean radiative energy budget. *Science* **295**, 841–844 (2002).
80. Trenberth, K. E. *et al.* Changes in tropical cloud and radiation. *Science Online* **296**, 2095a (2002).
81. Hurrell, J. W. Decadal trends in the North Atlantic Oscillation: regional temperatures and precipitation. *Science* **269**, 676–679 (1995).
82. Thompson, D. W. J. & Wallace, J. M. Annular modes in the extratropical circulation. *J. Clim.* **13**, 1000–1036 (2000).
83. Carnell, R. E. & Senior, C. A. An investigation into the mechanisms of changes in mid-latitude mean sea level pressure as greenhouse gases are increased. *Clim. Dynam.* **18**, 533–543 (2002).
84. Gillett, N. P. *et al.* How linear is the Arctic Oscillation response to greenhouse gases? *J. Geophys. Res.* **107**, 1029/2001JD000589 (2002).
85. Venzke, S., Allen, M. R., Sutton, R. T. & Rowell, D. P. The atmospheric response over the North Atlantic to decadal changes in sea surface temperature. *J. Clim.* **12**, 2562–2584 (1999).
86. Hoerling, M. P., Hurrell, J. W. & Xu, T. Y. Tropical origins for recent North Atlantic climate change. *Science* **292**, 90–92 (2001).
87. Corti, S. & Palmer, T. N. Sensitivity analysis of atmospheric low-frequency variability. *Q. J. R. Meteorol. Soc.* **123**, 2425–2447 (1997).
88. Ramaswamy, V. *et al.* in *Climate Change 2001: The Scientific Basis. Contribution of Working Group I to the Third Assessment Report of the Intergovernmental Panel on Climate Change* (eds Houghton, J. T. *et al.*) (Cambridge Univ. Press, Cambridge, 2001).
89. Seager, R. *et al.* Is the Gulf Stream responsible for europe’s mild winters? *Q. J. R. Meteorol. Soc.* (in the press).
90. Rahmstorf, S. On the freshwater forcing and transport of the North Atlantic Thermohaline Circulation. *Clim. Dynam.* **12**, 799–811 (1996).
91. Knutti, R. & Stocker, T. F. Limited predictability of the future thermohaline circulation close to an instability threshold. *J. Clim.* **15**, 179–186 (2002).
92. Smith, L. A. in *Nonlinear Dynamics and Statistics* (ed. Mees, A. I.) 31–64 (Birkhauser, Boston, 2001).
93. Hansen, J. A., Allen, M. R., Stainforth, D. A., Heaps, A. & Stott, P. A. Casino-21: climate simulation of the 21st century. *World Resource Rev.* **13**, 187–189 (2001).
94. Stainforth, D. *et al.* Distributed computing for public-interest climate modeling research. *Comput. Sci. Eng.* **4**, 82–89 (2002).
95. Mitchell, J. F. B., Johns, T. C. & Senior, C. A. The transient response to increasing greenhouse gases using models with and without flux adjustment. Tech. Rep. <www.metoffice.com/research/hadleycentre/pubs/HCTN> (1998).

Acknowledgements

We are grateful to G. Hegerl and K. Trenberth for thorough reviews; to J. Gregory, C. Forest, J. Mitchell, L. Smith and I. Tracey for helpful suggestions; and to B. Booth, B. Grey and H. Lambert for help with the figures. M. Webster, M. Hulme, P. Stott and J. Gregory kindly provided unpublished data used in Figs 1, 3 and 4, and we thank C. Covey and the CMIP-2 data team for data in Figs 2, 5 and 6. M.R.A. is supported by the UK NERC and US NOAA & DoE, W.J.I. by the UK Government Meteorological Research Programme and D.A.S. by the NERC COAPEC Programme. The www.climateprediction.net programme is funded by the UK NERC, EPSRC and DTI ‘e-Science’ programmes.

CORRIGENDUM

doi:10.1038/nature11456

Corrigendum: Constraints on future changes in climate and the hydrologic cycle

Myles R. Allen & William J. Ingram

Nature **419**, 224–232 (2002); doi:10.1038/nature01092

We thank P. Good for pointing out that the location of the transient runs (green diamonds) in Fig. 2 of this Insight is inconsistent with the text. With F_s positive downwards and κ positive, the sign of the third term in equation (2) (the hypothesized adjustment for disequilibrium) should be changed, giving:

$$\Delta R_C + k_T \Delta T + \kappa F_s = L \Delta P \quad (2)$$

The analysis and discussion are not affected.